

Properties and Reactions of Ketene in the Gas Phase by Ion Cyclotron Resonance Spectroscopy and Photoionization Mass Spectrometry. Proton Affinity, Site Specificity of Protonation, and Heat of Formation of Ketene

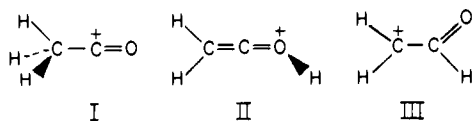
Jürgen Vogt,¹ Ashley D. Williamson, and J. L. Beauchamp*

Contribution No. 5594 from the Arthur Amos Noyes Laboratory
of Chemical Physics, California Institute of Technology,
Pasadena, California 91125. Received May 31, 1977

Abstract: The properties and reactions of ketene and ketene-*d*₂ are investigated using the techniques of ion cyclotron resonance spectroscopy and photoionization mass spectrometry. The major reaction sequence initiated by the ketene molecular ion in its ground vibrational state at thermal energies involves sequential incorporation of CH₂ into the ionic product with loss of CO. The species C₂H₃O⁺ (presumably the acyl cation) is a major product at long times or high pressure and does not react further with ketene neutrals. The energetics of ionization of ketene and ketene-*d*₂ and the effect of vibrational energy on reactivity are examined using photoionization mass spectrometry and photoelectron spectroscopy. The threshold determined for the endothermic process CH₂CO⁺ + CH₂CO → C₂H₄⁺ + 2CO provides confirmation of the recently redetermined heat of formation of ketene ($\Delta H_f^\circ = -11.4 \pm 0.4$ kcal/mol). Equilibrium proton transfer reactions in a number of mixtures lead to a determination of the proton affinity of ketene, PA(CH₂CO) = 195.9 ± 2 kcal/mol, relative to PA(NH₃) = 202.3 ± 2 kcal/mol. The site of protonation is shown to be the methylene carbon. These results yield $\Delta H_f^\circ(\text{CH}_3\text{CO}^+) = 159.9 \pm 2$ kcal/mol, which is discussed in light of other measurements of the heat of formation of the acyl cation. With sufficiently acidic species (e.g., CH₅⁺), oxygen protonation occurs.

The thermochemical properties and ion-molecule reactions of ketene in the gas phase have been investigated using the techniques of ion cyclotron resonance spectroscopy (ICR) and photoionization mass spectrometry (PIMS).² Previous studies of this interesting molecule include investigations of its molecular spectroscopy³⁻⁶ and an examination of thermal and photolytic dissociation reactions in the gas phase⁷ and have shown this species to be an unusually reactive substrate in solution.⁸ Because of the conjugated double bond, ketene has an unusual electronic structure.^{3-6,9-11} Particularly relevant to the present investigations are recent photolytic studies at selected wavelengths which revealed inconsistencies in the thermochemical data for CH₂ and ketene and led to a revision of the previously accepted value for the heat of formation of CH₂CO.¹² Calorimetric measurements by Rice and Greenberg¹³ in 1934 yielded a value of $\Delta H_f^{298}(\text{CH}_2\text{CO}) = -14.78$ kcal/mol. Nuttall et al.¹² recently noted that this value led to a predicted threshold of 3580 Å for the photolysis of ketene to yield CH₂ and CO. Since they had observed photolysis at wavelengths of up to 3690 Å, they repeated the calorimetric work of Rice and Greenberg, obtaining $\Delta H_f^{298}(\text{CH}_2\text{CO}) = -11.4 \pm 0.4$ kcal/mol. This is confirmed in the present work by relating the thermochemical properties of the ketene molecule and its reaction products through measurement of energy thresholds for endothermic ion-molecule reactions using photoionization mass spectrometry.¹⁴

Previous theoretical and experimental investigations of protonated ketene have considered the relative stabilities of the different isomers I-III.¹⁵⁻¹⁷ The conclusions of several



studies are that isomers II and III are, respectively, ~35 and 65 kcal/mol less stable than the acyl cation I.^{15,16} It has been noted that CH₃CO⁺ derived from acetone undergoes the proton-transfer reaction 1 with the parent neutral.¹⁷ This observation has been used to infer that the proton affinity of acetone, as well as other neutrals for which the same reaction is observed, is greater than that of ketene.¹⁷ In the present study, somewhat different conclusions are reached by examining the energetics of ketene protonation under equilibrium conditions. In addition, the site specificity of protonation is investigated briefly using proton donors of varying acidity. Ketene in solution protonates cleanly on the methylene carbon,¹⁸ and the structure of CH₃CO⁺ isolated as the hexafluoroantimonate salt has been reported.¹⁹

Experimental Section

The instrumentation and experimental techniques associated with ICR have been previously described.²⁰⁻²² The present experiments used an instrument built in Caltech shops which includes a 15-in. electromagnet capable of a maximum field strength of 23.5 kG. All experiments were performed at ambient temperature (25 °C).

The photoelectron spectrometer used in the present work has been previously described.²³ Ionization potentials are accurate to ±20 meV.²³ PIMS experiments were performed using the Caltech-Jet Propulsion Laboratory facility.²⁴ The light source for these experiments was the many-line spectrum of H₂. Entrance and exit slits were adjusted for a resolution of 1 Å. Repeller voltages used to extract ions from the differentially pumped ion source were typically 0.1 V. Photon intensities were measured using a cooled photomultiplier with a sodium salicylate scintillator coat. Over the narrow region scanned, the quantum efficiency of the scintillator was assumed constant. All experiments were performed at ambient temperature (25 °C).

Ketene was prepared by pyrolysis of acetic anhydride.²⁵ Unreacted acetic anhydride and acetic acid were condensed in a first trap immersed in a dry ice-acetone bath. Ketene was collected in a second trap cooled with liquid nitrogen and further purified by several trap-to-trap distillations. Ketene-*d*₂ was prepared in an analogous fashion from acetic anhydride-*d*₆ (99 at. % D). Analysis by mass spectrometric methods revealed no impurities. A trace of ketene dimer was observed in sample bulbs after several days.

Experimental Section

Results and Discussion

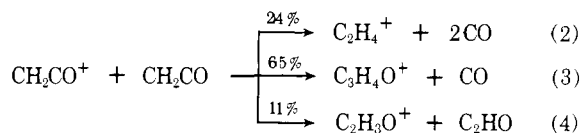
Ion-Molecule Reactions of Ketene. At low electron energy (16 eV), only the molecular ion of ketene is generated as an abundant species. The variation of ion abundance with time

Table I. Summary of Ion-Molecule Reaction Rate Constants

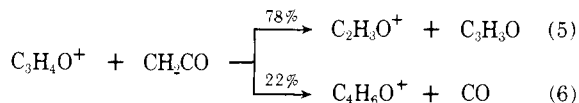
Process		Product distribution ^a	<i>k</i> ^b
CH ₂ CO ⁺ + CH ₂ CO	→ C ₂ H ₄ ⁺ + 2CO	0.24	5.9
	→ C ₃ H ₄ O ⁺ + CO	0.65	
	→ C ₂ H ₃ O ⁺ + C ₂ HO	0.11	
C ₃ H ₄ O ⁺ + CH ₂ CO	→ C ₂ H ₃ O ⁺ + C ₃ H ₃ O	0.78	1.6
	→ C ₄ H ₆ O ⁺ + CO	0.22	
CD ₂ CO ⁺ + CD ₂ CO	→ C ₂ D ₄ ⁺ + 2CO	0.20	5.9
	→ C ₃ D ₄ O ⁺ + CO	0.70	
	→ C ₂ D ₃ O ⁺ + C ₂ DO	0.10	
C ₃ D ₄ O ⁺ + CD ₂ CO	→ C ₂ D ₃ O ⁺ + C ₃ D ₃ O	0.54	2.0
	→ C ₄ D ₆ O ⁺ + CO	0.46	
(CD ₃) ₂ CO ⁺ + CH ₂ CO → (CD ₃) ₂ COCH ₂ ⁺ + CO			6.0
CH ₂ DCO ⁺ + CH ₂ CO → CH ₃ CO ⁺ + CHDCO			0.3 ^c

^a Product distributions measured at 16-eV electron energy. Distributions are a very sensitive function of the internal energy of the reactant ion (see text). ^b Total thermal rate constants, units 10⁻¹⁰ cm³ molecule⁻¹ s⁻¹, measured from limiting slope for disappearance of reactant ion. ^c Measured in mixture of CD₄ and CH₂CO. Reactions 18 and 19 lead to formation of CH₂DCO⁺.

shown in Figure 1 illustrates the reaction sequence initiated by this ion. Double resonance identifies reactions 2-4 as ac-



counting for the disappearance of CH₂CO⁺. The major product C₃H₄O⁺ undergoes reactions 5 and 6, with the ion



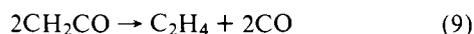
species C₄H₆O⁺ generated in the latter process reacting further as indicated in reaction 7. Reaction 7 is slow, and the minor



species C₅H₈O⁺, not shown in Figure 1, amounts to 3% of the total ionization at 200 ms. The species C₂H₃O⁺ does not react with the parent neutral. The ethylene molecular ion produced in process 2 reacts by charge transfer to regenerate the ketene molecular ion, reaction 8. Reactions 2 and 8 together comprise



a chain reaction which would result in the conversion of ketene to a mixture of ethylene and carbon monoxide (process 9) if it were not interrupted by reactions 3 and 4.



Reactions of ketene-*d*₂ confirm the proposed reaction pathways. This is necessary since C₂H₄ and CO have the same mass. For example, a product ion does not appear at *m/e* 48, which indicates that reaction 8 does not yield C₃H₆⁺, even though the process would be exothermic for either propylene or cyclopropane molecular ions. Reaction rates for the disappearance of the parent ions and major reaction products are given in Table I for both ketene and ketene-*d*₂.

Proton Affinity of Ketene. The proton affinity of ketene can be determined in trapped ion experiments by examining equilibria such as generalized in



The free energy of protonation is found to be between that of tetrahydrofuran and methyl acetate (Table II).²⁷ With both species double-resonance experiments indicate that the re-

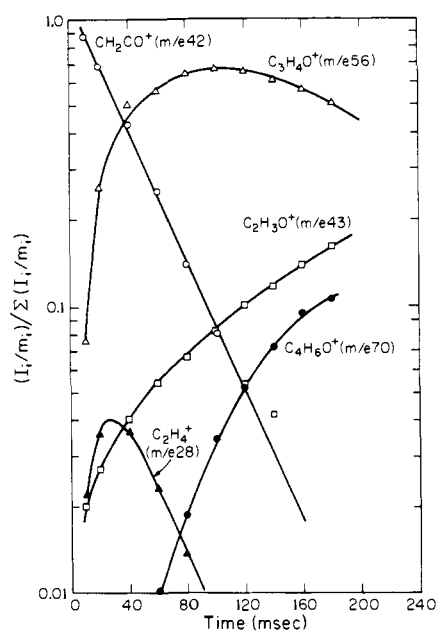


Figure 1. Variation of ion abundance with time in 1.3×10^{-6} Torr of ketene ionized by a 10-ms electron beam pulse at 16 eV.

versible proton-transfer reaction 10 is established. The relative free energies of protonation of methyl acetate, ketene, tetrahydrofuran, and acetone are summarized in Scheme I. The free

Scheme I

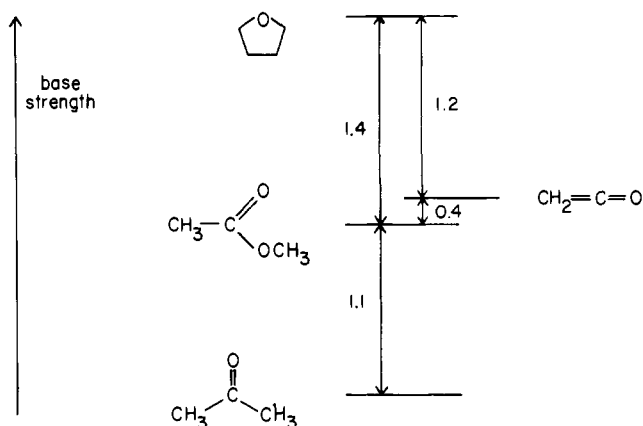


Table II. Proton Transfer Equilibria Involving Ketene

Equilibrium	K^a	ΔG°_{298} , kcal/mol	$\delta\Delta G^\circ_{298}$, ^b kcal/mol
$C_4H_8OH^+ + CH_2CO \rightleftharpoons CH_3CO^+ + C_4H_8O^c$	0.13	1.2	-5.9
$(CH_3CO_2CH_3)H^+ + CH_2CO \rightleftharpoons CH_3CO^+ + CH_3CO_2CH_3$	2.0	-0.4	-5.7

^a Equilibrium constant measured at ~298 K. Reported values are average of at least three determinations. ^b Free energy of protonation of ketene relative to ammonia. A minus sign indicates a species less basic than ammonia. Data for tetrahydrofuran and methyl acetate are from ref 26. ^c Tetrahydrofuran.

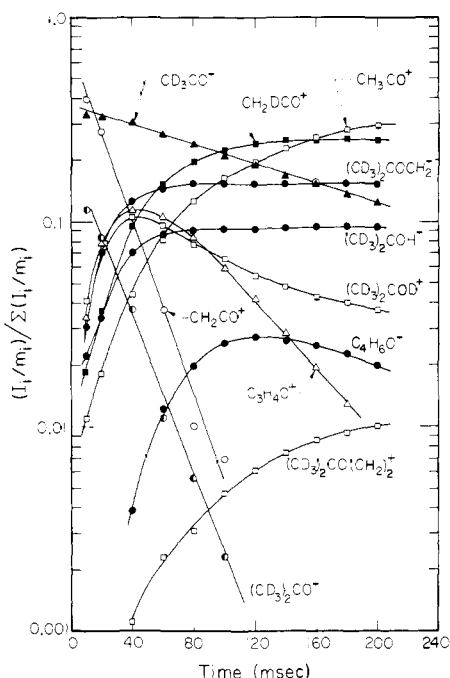
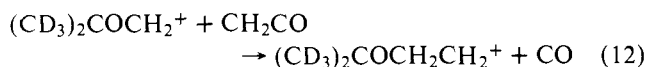
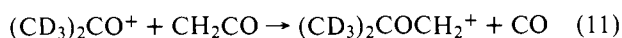


Figure 2. Variation of ion abundance with time for the major ionic species observed in a 1:1 mixture of ketene and acetone- d_6 at 4.6×10^{-6} Torr total pressure. Ionization is initiated with a 10-ms 16-eV electron beam pulse.

energy of protonation of ketene is thus determined to be 5.8 ± 0.2 kcal/mol less than NH_3 . Correcting the entropy effects due to changes in symmetry numbers gives an enthalpy of protonation 6.4 kcal/mol less than NH_3 . Using $PA(NH_3) = 202.3 \pm 2$ kcal/mol,²⁸ this gives $PA(CH_2CO) = 195.9 \pm 2$ kcal/mol. This is somewhat less than the theoretical predictions of 217 kcal/mol¹⁸ and 202 kcal/mol.¹⁶ Using $\Delta H_f(CH_2CO) = -11.4 \pm 0.4$ kcal/mol,¹² the measured proton affinity gives $\Delta H_f(CH_3CO^+) = 159.9 \pm 2$ kcal/mol. This is in excellent agreement with the value $\Delta H_f(CH_3CO^+) = 157.8$ kcal/mol recently measured in our laboratory using photoionization mass spectrometry and confirmed in studies of halide transfer equilibria.²⁹

As noted in the introduction, observation of reaction 1 in acetone has been used to infer that the proton affinity of acetone is higher than that of ketene,¹⁷ which contrasts with the present results (Scheme I) which indicate the reverse. The present results are confirmed by the data shown in Figure 2 for the variation of ion abundance with time in a mixture of acetone- d_6 and ketene. The acetone molecular ion reacts with ketene by sequential methylene addition (reactions 11 and 12, yielding products at m/e 78 and 92). The fragment ion



CD_3CO^+ (m/e 46) reacts with both ketene and acetone by

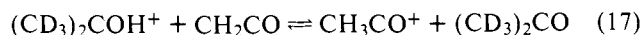
deuteron transfer (processes 13 and 14). Double-resonance



experiments identify processes 15 and 16 which eventually lead



to all of the labile deuterium being lost to neutral molecules.³⁰ Despite the complexity of the reaction sequence, the equilibrium proton-transfer reaction 17 is being established at long

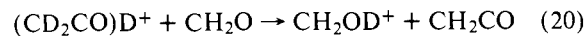


times and clearly lies to the right ($\Delta G^\circ = -1.4$ kcal/mol corresponds to $K = 10$, which is approximately what is observed at long times).

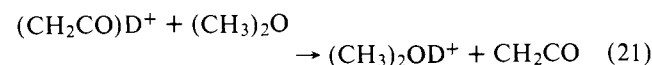
The dipole moment of ketene is 1.41 D with oxygen being the negative end of the dipole.³¹ If energetically feasible, protonation on oxygen should thus be a facile process.³² Electron-impact ionization of CD_4 leads to formation of CD_3^+ and CD_4^+ which react with CD_4 to yield $C_2D_5^+$ and CD_5^+ , respectively. The proton affinities of ethylene and methane are ~160 and 126 kcal/mol, respectively.²⁰ Hence both reactions



observed when ketene is added to excess CD_4 , could result in oxygen protonation. The species $(CH_2CO)D^+$ in this system reacts slowly ($k \approx 3 \times 10^{-11}$ cm³ molecule⁻¹ s⁻¹) with CH_2CO in accordance with reaction 16 observed in the mixture of acetone- d_6 with ketene. This process can itself be taken as evidence for the favored (but not exclusive) site of protonation being on the methylene carbon.³⁰ Addition of formaldehyde to the mixture of ketene and CD_4 results in the formation of CH_2OD^+ . Continuous ejection of m/e 44, corresponding to $(CH_2CO)D^+$, does not lead to a decrease in the abundance of CH_2OD^+ (i.e., reaction 20 does not occur). With



dimethyl ether, however, ejection of m/e 44 leads to a substantial decrease in the observed abundance of $(CH_3)_2OD^+$, thus identifying reaction 21. These results are consistent with



the existence of a second isomer, namely II, with the oxygen site having a proton affinity between $PA(CH_2O) = 175$ kcal/mol and $PA((CH_3)_2O) = 190$ kcal/mol.³² Hence the methylene carbon is more basic than oxygen by 18 ± 8 kcal/mol. This is somewhat smaller than the theoretical predictions^{15,16} of ~35 kcal/mol.

Photoionization Studies. The energetics of the sequence of reactions 2 and 8 which result in the overall conversion of ke-

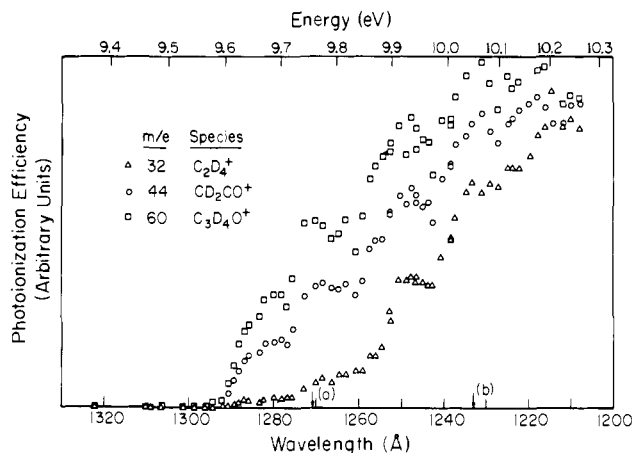


Figure 3. Photoionization efficiency of molecular ion and product ions of reactions 2 and 3 in ketene- d_2 . Arrows indicate thresholds calculated for reaction 2 using (a) data of Nuttall et al.,¹² (b) data of Rice and Greenberg.¹³

Table III. Thermochemistry of Reactions 2, 8, and 9

Reaction	ΔH_f^a kcal/mol	
	NLK ^b	RG ^c
$\text{CH}_2\text{CO}^+ + \text{CH}_2\text{CO} \rightarrow \text{C}_2\text{H}_4^+ + 2\text{CO}$	3.3	10.1
$\text{C}_2\text{H}_4^+ + \text{CH}_2\text{CO} \rightarrow \text{CH}_2\text{CO}^+ + \text{C}_2\text{H}_4$	-20.8	-20.8
$2\text{CH}_2\text{CO} \rightarrow \text{C}_2\text{H}_4 + 2\text{CO}$	-17.5	-10.7

^a Except as noted in the text, data are from J. L. Franklin, J. A. Dillard, H. M. Rosenstock, J. T. Herron, K. Draxl, and F. H. Field, *Natl. Stand. Ref. Data Ser., Natl. Bur. Stand.*, No. 26 (1969).
^b Using $\Delta H_f^{298}(\text{CH}_2\text{CO}) = -11.4$ kcal/mol.¹² ^c Using $\Delta H_f^{298}(\text{CH}_2\text{CO}) = -14.8$ kcal/mol.¹³

tene to ethylene and carbon monoxide (process 9) are summarized in Table III. The data of Nuttall et al.,¹² predict the enthalpy of reaction 2 to be 3.1 kcal/mol; the older data of Rice and Greenberg¹³ give 10.1 kcal/mol for the same quantity. The enthalpy change for reaction 2 involving ketene- d_2 can be calculated. Since photoionization measurements indicate no significant isotope effect on the ionization potential of ketene or ethylene,³³ the thermodynamic isotope effect on ion-molecule reaction 1 is identical with that of its neutral analogue. This quantity was estimated using the vibrational frequencies of Moore and Pimentel³⁴ for ketene and ketene- d_2 and those of Arnett and Crawford³⁵ for ethylene and ethylene- d_4 . As a result, the enthalpy of reaction 2 was found to be 0.14 kcal/mol less for ketene- d_2 than for ketene itself.

The preceding data suggest a sensitive test to distinguish the two reported values for the heat of formation of ketene. Theories of ion-molecule reaction dynamics³⁶ predict that increased internal energy in the reactants will lead to a decrease in the cross section for exothermic reaction channels. At 0 K, the cross sections of endothermic channels will show an onset at an energy equal to the reaction endothermicity and will increase with internal energy. At 298 K, the thermal energy of the reactants will result in a nonzero cross section below the 0 K threshold, but the qualitative behavior of the cross section will not be altered. These expectations have been experimentally verified for reactions of rare gas atoms with hydrogen molecular ions.^{36,37} Thus the cross section of reaction 2 as a function of the internal energy of the reactant should exhibit a sharp increase in the vicinity of threshold. The threshold thus determined may be used to calculate the heat of formation of ketene.

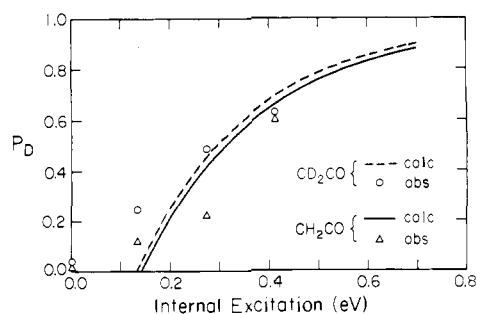


Figure 4. Comparison of calculated and observed probabilities for sequential decomposition of the activated complexes formed by reaction of ketene molecular ions with ketene. The quantity $\sigma_2/(\sigma_2 + \sigma_3)$ is used as an experimental measure of P_D . The energy scale refers to the internal energy of the reactant ion.

The photoelectron spectrum of ketene reveals the internal energy states of the parent ion which are accessible by direct photoionization. Spectra taken in our laboratory exhibit a vibrational progression in the ground electronic state with frequency 2240 ± 80 cm^{-1} for both isotopic species, and a second progression of the same frequency offset by 1090 ± 80 cm^{-1} . Since neither vibration exhibits an isotopic shift, Turner's³⁸ assignments of the major vibration as the C-O stretch ν_2 and the minor vibration as the C-C stretch ν_4 seem reasonable. Our spectra differ from Turner's only in that his value of 9.64 eV for the adiabatic ionization potential of ketene³⁸ does not agree with our value of 9.61 ± 0.02 eV by photoelectron spectroscopy or 9.614 ± 0.008 eV for both isotopic species by photoionization mass spectrometry.

The photoionization efficiency of the parent ion in ketene- d_2 is shown in circles in Figure 3. The states found in the photoelectron spectrum occur as distinct steps in Figure 3, suggesting that direct ionization rather than autoionization predominates in this system. Also shown in Figure 3 are the products of reactions 2 and 3. The vertical arrows in Figure 3 correspond to calculated thresholds for reaction 2 using the differing values of the heat of formation of ketene.

Using the assumption that the height of each step in the photoionization efficiency curve is proportional to the number of ions formed in the corresponding vibrational level, relative cross sections for reactions 2-4 have been calculated for both isotopic species and are summarized in Table IV. As is evident from Figure 3 and Table IV, the cross section for reaction 2 is small for ground-state ketene ions and increases by an order of magnitude as vibrational energy is added to the reactant ion. In contrast the cross section for reaction 3 decreases slightly, as is often observed for an exothermic reaction which is rapid at thermal energies. The data in Figure 4 and Table IV are clearly consistent with the data of Nuttall et al.¹² and do not support the earlier study.¹³

The ion-neutral collision rate for the molecular ion in ketene computed by the theory of Gioumousis and Stevenson¹⁸ is 1.0×10^{-9} cm^3 molecule⁻¹ s⁻¹, which is a lower limit to the true collision rate due to the permanent dipole moment of ketene.³² Comparison with the total rate measured in our ICR study (Table I) shows that reaction does not occur in at least 40% of the encounters. The data in Table IV indicate that the total cross section for reactions 2-4 remains approximately constant over the internal energy range studied. The probability of unreactive collisions is essentially unaffected in comparison with changes in the product distribution. This constancy of the total reaction probability suggests that the observed variation of cross sections with vibrational energy is due to competition among the various reaction channels. Furthermore, unless there exists some concerted route to eliminate two CO species simultaneously from the intermediate complex, CO elimination must occur in a stepwise manner; that is, the products of re-

Table IV. Cross Sections for Reactions 2-4 for Lower Vibrational Levels of Reactant Ion^a

Vibrational state			Reactions in CD ₂ CO				Reactions in CH ₂ CO ^c		
ν_2	ν_4	Vibrational energy ^b	σ_2	σ_3	σ_4	σ_{total}	σ_2	σ_3	σ_{total}
0	0	0.0	0.04	1.00	0.04	1.08	0.02	1.00	1.02
0	1	0.13	0.24	0.71	0.03	0.98	0.09	0.68	0.77
1	0	0.27	0.65	0.67	0.06	1.28	0.22	0.72	0.94
1	1	0.41	0.82	0.50	0.07	1.39	0.59	0.37	0.96

^a Cross sections are normalized relative to σ_3 for ground-state reactant ions; product yields were measured at low conversion to avoid higher order reactions and with low repeller voltages (0.1 V) to avoid reactant ions with high translational energy. ^b Energies in electronvolts. For given values of ν_2 and ν_4 , the vibrational energies of CD₂CO⁺ and CH₂CO⁺ are identical within experimental error. ^c Cross section for reaction 4 was not calculated owing to interference from ¹³C isotope peak of parent ion at the same mass.

Table V. Summary of Thermochemical Data for Ketene, Diazomethane, and Their Conjugate Acids^a

Species (B)	Conjugate acid (BH ⁺)	$\Delta H_f(\text{B})$	$\Delta H_f(\text{BH}^+)$	IP(B)	PA(B)	$D(\text{B}^+-\text{H})$
CH ₂ CO	CH ₃ CO ⁺	-11.4 ± 0.4^b	159.9 ± 2^c	9.61^c	195.9 ± 2^c	103.9 ± 2^d
CH ₂ N ₂	CH ₃ N ₂ ⁺	55 ± 4^e	209.4 ± 2^f	9.00^g	213 ± 5^h	107 ± 5^d

^a All data are given in kilocalories/mole at 298 K except ionization potentials, which are given in electronvolts. ^b Reference 12. ^c This work. ^d Calculated using eq 25. ^e Reference 47. ^f Reference 46. ^g Table III, ref *a*. ^h Calculated as indicated in text.

action 2 must arise from decomposition of C₃H₄O⁺ formed with excess internal energy.

In accordance with the RRKM theory of unimolecular reactions, the fraction of [C₃H₄O₂⁺][‡] activated complexes in which the product C₃H₄O⁺ retains sufficient internal excitation in excess of the critical energy E_c for the second decomposition is given by the approximate equation

$$P_D = \frac{\int_0^{E^\ddagger - E_c} N(E^\ddagger - E_t^\ddagger) dE_t^\ddagger}{\int_0^{E^\ddagger} N(E^\ddagger - E_t^\ddagger) dE_t^\ddagger} \quad (22)$$

where $N(E^\ddagger - E_t^\ddagger)$ is the density of internal states in the critical configuration at energy $E^\ddagger - E_t^\ddagger$, E^\ddagger is the total vibrational and translational energy of the products, and E_t^\ddagger is the final relative translational energy of the products.⁴⁰⁻⁴² For simplicity, the rotational energy of the complex is ignored. P_D can be evaluated in a straightforward manner, giving

$$P_D = 1 - \frac{W(E_c)}{W(E^\ddagger)} \quad (23)$$

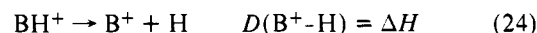
in terms of $W(E)$, the total number of states of the activated complex with energy $\leq E$. Using the Whitten-Rabinovitch⁴³ approximation for energy level sums, the predictions of eq 23 are compared with the experimental results in Figure 4.⁴⁴ For the calculation shown, the effective number of oscillators chosen is $s_{\text{eff}}^\ddagger = 11$. Equation 23 correctly predicts that P_D increases rapidly with increasing vibrational energy above threshold and that with the same internal excitation the extent of decomposition of the deuterated complex is greater, even when the same E_c is used for both complexes. Although the direction of the effect is correct, the observed isotope effect is larger than calculated. The calculation ignores the contribution of thermal energy (initial relative translational energy and internal energy) to decomposition near threshold. Considering that the range of internal excitation over which P_D increases rapidly is small (~ 0.2 eV) compared with E_c (1.26 eV), there is no evidence for a significantly greater release of internal energy to translation than is expected from the RRKM analysis.

Conclusion

Ketene is observed to transfer CH₂ to radical cations as the major reaction sequence in ketene and in mixtures with other species (e.g., reaction 11 involving CH₂ addition to the molecular ion of acetone). Curiously, however, this process is not observed with even electron ions. In both cases the reactions are significantly exothermic owing to the weak bond between

CH₂ and CO (77 kcal/mol). This process could be used to generate some interesting species for further study. For example, the reaction of formaldehyde molecular ions with ketene should lead to the formation of CH₂OCH₂⁺ (ring-opened ethylene oxide), which is predicted to be the most stable C₂H₄O⁺ isomer.²⁴

The electron donor ability or base strength of the oxygen site in ketene is greatly reduced by involvement of the oxygen lone pairs in π bonding with carbon. Whereas only the out-of-plane orbital of aldehydes and ketones is involved in π bonding, ketene is unusual in that both p- π orbitals participate in π -bond formation. The highest occupied molecular orbital, 2b₁, is π bonding with amplitude mainly on the methylene carbon.^{9,10} Previously we have shown that the energy of the orbital involved in bond formation to the approaching proton, as measured by the ionization potential, can be correlated with the homolytic bond dissociation energy (defined by the enthalpy change for process 24).^{20,23,45}



The expression

$$D(\text{B}^+-\text{H}) = \text{PA}(\text{B}) + \text{IP}(\text{B}) - \text{IP}(\text{H}) \quad (25)$$

relates the homolytic bond dissociation energy, $D(\text{B}^+-\text{H})$, to the proton affinity of a species B, with IP(B) referring to the adiabatic ionization potential. Specifically, it has been shown that the quantities $D(\text{B}^+-\text{H})$ are either constant or exhibit systematic trends within a homologous series.^{23,45} With this in mind, it is of interest to compare the carbon-hydrogen homolytic bond dissociation energies of the conjugate acids of ketene and diazomethane (Table V). The heat of formation of CH₃N₂⁺ has recently been determined by photoionization mass spectrometry, which gives $\Delta H_f(\text{CH}_3\text{N}_2^+) = 209.4 \pm 1.9$ kcal/mol.⁴⁶ Laufer and Okabe have reviewed various determinations of $\Delta H_f(\text{CH}_2\text{N}_2)$ and arrive at the conclusion that it is within the limits $51 < \Delta H_f(\text{CH}_2\text{N}_2) \leq 60$ kcal/mol.⁴⁷ Using $\Delta H_f(\text{CH}_2\text{N}_2) = 55 \pm 4$ kcal/mol gives $\text{PA}(\text{CH}_2\text{N}_2) = 213 \pm 5$ kcal/mol, making diazomethane a significantly stronger base than ketene. Within experimental error, however, the C-H homolytic bond dissociation energies in the conjugate acids, 104 kcal/mol for ketene and 107 kcal/mol for diazomethane (Table IV), are equal. The measured bond dissociation energies are ~ 8 kcal/mol higher than a normal primary C-H bond. In general, bond dissociation energies in ions tend to be higher than in the isoelectronic neutrals.²⁰ Although it remains controversial, the C-H bond dissociation energy in

CH₃CN, which is isoelectronic with CH₃CO⁺ and CH₃N₂⁺, is almost certainly <104 kcal/mol.⁴⁸

Acknowledgments. This research was supported in part by the U.S. Energy Research and Development Administration, under Grant No. E(04-3)767-8, and by the National Aeronautics and Space Administration, under Contract No. NAS7-100. The PIMS instrumentation was made possible by a grant from the President's Fund of the California Institute of Technology. One of us (J.V.) thanks the Kanton Basel-Stadt, Switzerland, for a paid leave of absence.

References and Notes

- (1) Postdoctoral Fellow, 1974–1975, on leave from Physikalisches Chemisches Institut der Universität, Basel, Switzerland.
- (2) For a brief summary of part of this work, see A. D. Williamson, J. Vogt, and J. L. Beauchamp, *Chem. Phys. Lett.*, **47**, 330 (1977).
- (3) For a review of early work, see J. W. Rabalais, J. M. McDonald, V. Scherr, and S. P. McGlynn, *Chem. Rev.*, **71**, 73 (1971).
- (4) A. H. Laufer and R. A. Keller, *J. Am. Chem. Soc.*, **93**, 61 (1971).
- (5) J. Vogt, M. Jungen, and J. L. Beauchamp, *Chem. Phys. Lett.*, **40**, 500 (1976).
- (6) R. P. Frueholz, W. M. Flicker, and A. Kuppermann, *Chem. Phys. Lett.*, **38**, 57 (1976).
- (7) J. W. Simons and B. S. Rabinovitch, *J. Phys. Chem.*, **68**, 1322 (1964); S.-Y. Ho and W. A. Noyes, *J. Am. Chem. Soc.*, **89**, 5091 (1967); B. A. DeGraff and G. B. Kistiakowsky, *J. Phys. Chem.*, **71**, 3984 (1967); G. B. Kistiakowsky and T. A. Walter, *ibid.*, **72**, 3952 (1968); A. N. Strachan and D. E. Thornton, *Can. J. Chem.*, **46**, 2353 (1968); W. Braun, A. M. Bass, and M. Pilling, *J. Chem. Phys.*, **52**, 5131 (1970); K. Dees, D. W. Setser, and W. G. Clark, *J. Phys. Chem.*, **75**, 2231 (1971); K. Dees and D. W. Setser, *ibid.*, **75**, 2240 (1971); V. Zabransky and R. W. Carr, Jr., *ibid.*, **79**, 1618 (1975).
- (8) D. J. Cram and G. S. Hammond, "Organic Chemistry", 2nd ed, McGraw-Hill, New York, N.Y., 1964.
- (9) J. E. Del Bene, *J. Am. Chem. Soc.*, **94**, 3713 (1972).
- (10) C. E. Dykstra and H. F. Schaefer III, *J. Am. Chem. Soc.*, **98**, 2689 (1976).
- (11) L. B. Harding and W. A. Goodard III, unpublished work.
- (12) R. L. Nuttall, A. H. Laufer, and M. V. Kilday, *J. Chem. Thermodyn.*, **3**, 167 (1971).
- (13) F. O. Rice and J. Greenberg, *J. Am. Chem. Soc.*, **56**, 2268 (1934).
- (14) For a general review of the technique, see W. A. Chupka in "Ion-Molecule Reactions", J. L. Franklin, Ed., Plenum Press, New York, N.Y., 1972.
- (15) A. C. Hopkinson, *J. Chem. Soc., Perkin Trans. 2*, 795 (1973).
- (16) D. R. Yarkony and H. F. Schaefer III, *J. Chem. Phys.*, **63**, 4317 (1975).
- (17) J. Long and B. Munson, *J. Am. Chem. Soc.*, **95**, 2427 (1973).
- (18) G. A. Olah, K. Dunne, Y. K. Mo, and P. Szilagy, *J. Am. Chem. Soc.*, **94**, 4200 (1974).
- (19) F. P. Boer, *J. Am. Chem. Soc.*, **90**, 6706 (1968).
- (20) J. L. Beauchamp, *Ann. Rev. Phys. Chem.*, **22**, 527 (1971).
- (21) T. B. McMahon and J. L. Beauchamp, *Rev. Sci. Instrum.*, **43**, 509 (1972).
- (22) M. K. Murphy and J. L. Beauchamp, *J. Am. Chem. Soc.*, **98**, 5781 (1976).
- (23) For a recent application of this instrumentation, see R. H. Staley, J. E. Kleckner, and J. L. Beauchamp, *J. Am. Chem. Soc.*, **98**, 2018 (1976).
- (24) For recent applications of this instrumentation in studying ion-molecule reactions, see R. R. Corderman, P. R. LeBreton, S. E. Buttrill, Jr., A. D. Williamson, and J. L. Beauchamp, *J. Chem. Phys.*, **65**, 4929 (1976).
- (25) The preparation follows that given in *Org. Syn.*, **45**, 50 (1965).
- (26) J. F. Wolf, R. H. Staley, I. Koppel, M. Taagepera, R. T. McIver, Jr., J. L. Beauchamp, and R. W. Taft, *J. Am. Chem. Soc.*, **99**, 5417 (1977).
- (27) Data other than those presented in Table II are taken from ref 29. See also, R. W. Taft, "Proton Transfer Reactions", E. F. Caldin and V. Gold, Ed., Chapman and Hall, London, 1975.
- (28) Reference data for absolute proton affinities can best fit the relative proton affinities in ref 29 by assuming PA(NH₃) = 202.3 ± 2 kcal/mol (J. L. Beauchamp, R. H. Staley, S. E. Buttrill, J. F. Wolf, and R. W. Taft, unpublished work). See also R. Yamdagni and P. Kebarle, *J. Am. Chem. Soc.*, **98**, 1320 (1976).
- (29) R. H. Staley, R. D. Wieting, and J. L. Beauchamp, *J. Am. Chem. Soc.*, **99**, 5964 (1977); earlier studies of ΔH_f(CH₃CO⁺) are discussed in this paper.
- (30) Related processes and their implications are discussed by T. B. McMahon and J. L. Beauchamp, *J. Phys. Chem.*, **81**, 593 (1977).
- (31) H. R. Johnson and M. W. Strandberg, *J. Chem. Phys.*, **18**, 687 (1952).
- (32) T. Su and M. T. Bowers, *J. Chem. Phys.*, **58**, 3027 (1973).
- (33) R. Botter, V. H. Dibeler, J. A. Walker, and H. M. Rosenstock, *J. Chem. Phys.*, **45**, 1198 (1966).
- (34) C. B. Moore and G. Pimentel, *J. Chem. Phys.*, **38**, 2816 (1963).
- (35) R. L. Arnett and B. L. Crawford, Jr., *J. Chem. Phys.*, **18**, 118 (1950).
- (36) J. C. Light, *J. Chem. Phys.*, **40**, 3221 (1964); J. C. Light and J. Lin, *ibid.*, **43**, 3209 (1965).
- (37) W. A. Chupka and M. E. Russell, *J. Chem. Phys.*, **49**, 5426 (1968).
- (38) D. W. Turner, C. Baker, A. D. Baker, and C. R. Brundle, "Molecular Photoelectron Spectroscopy", Wiley-Interscience, London, 1970.
- (39) G. Gioumousis and D. P. Stevenson, *J. Chem. Phys.*, **29**, 294 (1958).
- (40) P. J. Robinson and K. A. Holbrook, "Unimolecular Reactions", Wiley-Interscience, London, 1972.
- (41) S. A. Safran, N. D. Weinstein, D. R. Herschbach, and J. C. Tully, *Chem. Phys. Lett.*, **12**, 564 (1972).
- (42) A. Lee, R. L. Leroy, F. Herman, R. Wolfgang, and J. C. Tully, *Chem. Phys. Lett.*, **12**, 569 (1972).
- (43) G. F. Whitten and B. S. Rabinovitch, *J. Chem. Phys.*, **38**, 2466 (1963).
- (44) A loose complex was assumed in which the vibrational frequencies of ketene appear twice with the addition of five low frequencies to describe the additional modes of the complex. The latter are not critical in the calculation. Frequencies for ketene and ketene-d₂ were taken from ref 34 and W. F. Arendale and W. H. Fletcher, *J. Chem. Phys.*, **26**, 793 (1957). For both cases a frequency of 900 cm⁻¹ was excluded as the reaction coordinate. The parameters in the Whitten-Rabinovitch treatment were E₂ = 1.931 eV and β = 1.410 for the CH₂CO system and E₂ = 1.613 eV and β = 1.341 for CD₂CO.
- (45) R. H. Staley, M. Taagepera, W. G. Henderson, J. L. Beauchamp, and R. W. Taft, *J. Am. Chem. Soc.*, **99**, 326 (1977).
- (46) M. S. Foster, A. D. Williamson, and J. L. Beauchamp, *Int. J. Mass Spectrom. Ion Phys.*, **15**, 429 (1974).
- (47) A. H. Laufer and H. Okabe, *J. Am. Chem. Soc.*, **93**, 4137 (1971).
- (48) D. J. Bogan and D. W. Setser, *J. Chem. Phys.*, **64**, 586 (1976).

Photoreduction and Photodecarboxylation of Pyruvic Acid. Applications of CIDNP to Mechanistic Photochemistry

G. L. Closs* and R. J. Miller

Contribution from the Department of Chemistry, The University of Chicago, Chicago, Illinois 60637. Received September 26, 1977

Abstract: Detailed mechanisms for the reduction of n,π* triplet pyruvic acid by ethanol, 2-propanol, and acetaldehyde in acetonitrile solution have been elucidated by CIDNP. Various geminate combination and disproportionation reactions, including the general formation of pyruvic acid enol (7), are observed. The significance of escape reactions involving hydrogen exchange between ketyl radicals and ground-state pyruvic acid is demonstrated. With moderate concentrations of ethanol, competitive abstraction from product acetaldehyde becomes important. Photodecarboxylation of n,π* triplet pyruvic acid in water and other nonreducing, polar solvents is initiated via unimolecular scission of the carbonyl-carboxy bond. Rapid reduction of ground-state pyruvic acid by carboxyl radicals followed by radical coupling yields 2-hydroxy-2-methylacetoacetic acid (8) as the primary photoproduct in all solvents. The rate coefficient for α-cleavage in acetonitrile solution is estimated to be 1 × 10⁶ s⁻¹. All observations are well explained with the radical pair theory of CIDNP.

The photophysical and photochemical properties of α-ketocarboxylic acids are not well understood.¹ While it has long been known that irradiation of aqueous solutions of pyruvic acid (1) afford high yields of acetoin (eq 1),² this interesting

transformation has stimulated only coarse mechanistic conjecture (eq 2)³ rationalized by presumed analogy to vapor-phase results.⁴

Pyruvic acid is efficiently photoreduced in the presence of